MEASUREMENT OF THE CROSS-SECTION RATIO σ_n/σ_p IN INELASTIC MUON-NUCLEON SCATTERING AT VERY LOW x AND Q^2 *

Vassili Papavassiliou
Physics Division
Argonne National Laboratory
9700 South Cass Avenue
Argonne, Illinois 60439-4828

ANL/PHY/CP--77536

DE93 002916

(Representing the Fermilab E-665 Collaboration)

Abstract

Preliminary results are presented on the measurement of the cross-section ratio σ_n/σ_p in inelastic μN scattering obtained by the E-665 experiment using the Fermilab 490 GeV/c muon beam and liquid H_2 and D_2 targets. The results extend the previously measured x range by two orders of magnitude, down to 2×10^{-5}, at $Q^2 > 10^{-2}\text{GeV}^2/c^2$. The ratio is consistent with 1 throughout the new range.

INTRODUCTION

Recently, there has been considerable interest in the very small x ($x < 10^{-2}$) behaviour of the nucleon structure functions (where x is the Bjorken scaling variable), soon to be probed at HERA. Theoretical calculations based on Perturbative Quantum Chromodynamics (PQCD) make interesting predictions for this kinematic range.[1,2] In current fixed-target experiments, the low-x region can be accessed only at the expense of low Q^2 ($Q^2 < 1$ GeV$^2/c^2$), where PQCD is not applicable. Here Q^2 is the invariant mass squared of the virtual photon that mediates the interaction. This kinematic range is frequently studied using Regge theory. A recent study[3] gives predictions for the structure functions of the nucleon at low x down to $Q^2 = 0$, extrapolating from data at higher Q^2.

Recent data[4] on the proton and neutron structure functions F_2^p and F_2^n cover the range $x > 0.008$, $Q^2 > 0.75$ GeV$^2/c^2$. The ratio F_2^n/F_2^p has been measured[5] down to $x = 0.002$ and is seen approaching 1 at the lowest x values. Similarly, data[6] on the total real-photon ($Q^2 = 0$) absorption cross sections on H_2 and D_2 show that the proton and neutron cross sections differ by only a few percent in the range $\nu = 4 - 18$ GeV, where ν is the photon energy in the laboratory frame, approaching a common value at large ν.

This paper presents preliminary results on the ratio of inelastic cross sections σ_n/σ_p in muon-nucleon scattering that include, for the first time, the range $x = 2 \times 10^{-5} - 2 \times 10^{-3}$, with $Q^2 > 0.01$ GeV$^2/c^2$ and $\nu > 50$ GeV, obtained by Fermilab experiment E-665. This ratio is equal to the ratio F_2^n/F_2^p, under some assumptions, to be discussed at the end.

THE EXPERIMENT

Data were taken in the Fermilab muon beam using the E-665 double-dipole open-geometry spectrometer[7] during the 1987–88

*This work supported in part by the U.S. Department of Energy, Nuclear Physics Division under contract W-31-109-ENG-38.

DISCLAIMER

fixed-target run. The relevant data for this analysis were taken on two 1.1 m-long liquid targets, a D_2 target (density 0.16 g/cm^2) and a H_2 target (0.07 g/cm^2), at 490 GeV/c mean beam momentum. The Small-Angle Trigger (SAT)[7] triggered on the absence of a veto signal at the expected position of the unscattered beam, determined by a processor for each incoming beam track, detected in a set of 7 scintillator planes. The acceptance of the trigger extended to scattering angles smaller than 0.1 mrad, inside the phase space of the unscattered beam.

The scattered muon was identified in the off-line analysis by its ability to penetrate a set of steel and concrete absorbers; its trajectory was reconstructed with the help of proportional and drift chambers. An electromagnetic calorimeter was used to discriminate between electrons and hadrons and to detect neutral particles depositing electromagnetic energy.

EVENT SELECTION

Events were selected requiring both the incoming and scattered muon tracks to be fully reconstructed and fitted to a vertex with a χ^2 probability better than 10^{-3} within the fiducial volume of the target. The following kinematic cuts were applied to constrain the data sample away from regions where the resolution in the kinematic variables is poor or the radiative corrections are too large:

$$\begin{gathered} E_B > 400 \text{ GeV} \\ Q^2 > 10^{-2} \text{ GeV}^2/c^2 \\ x > 2 \times 10^{-5} \\ 0.1 < y < 0.9 \\ \nu > 50 \text{ GeV} \\ |\phi - \pi| > 0.2 \text{ rad} \end{gathered}$$

Here E_B is the beam energy, the photon energy ν is the energy transfer in the laboratory, $y = \nu/E_B$ is the fractionai energy transfer and ϕ is the azimuthal angle of the scattered muon around the incoming muon direction. This last cut eliminated events with the outgoing muon in the horizontal (bending) plane, for which the vertex was poorly determined. The resolution in x is approximately constant at $\sim 15\%$ for $x > 0.001$ but this value increases to about 50% at the lowest x.

Rejection of electromagnetic backgrounds

In addition to the above cuts, two independent methods were employed to separate inelastic events from the large electromagnetic backgrounds, not related to the nucleon structure, that dominate at $x < 10^{-3}$. These backgrounds are due to elastic μe scattering in the target and to muon bremsstrahlung. The first type appears as a peak in the x distribution centered at $x = m_e/m_p \approx 5 \times 10^{-4}$, where m_e and m_p are the electron and proton masses, respectively, with a width determined by the experimental resolution. The second background type appears as events with large energy loss (ν) reconstructed with very small scattering angles and therefore at very low x. Figure 1 shows the event distribution in $\log_{10} x$ after the kinematic cuts (solid line).

In the first method, electromagnetic events were rejected by selecting only those events for which the total electromagnetic energy E_{CAL} deposited in the calorimeter was less than 0.4ν, or for which the bremsstrahlung planarity was greater than 10^{-5}. This quantity is defined from the momentum vectors p and p$'$ of the incoming and outgoing muons and the vector k connecting the vertex to the largest-energy cluster on the calorimeter, as

$$\mathcal{P} = \frac{|(\mathbf{p} \times \mathbf{p}') \cdot \mathbf{k}|}{|\mathbf{p}||\mathbf{p}'||\mathbf{k}|}. \qquad (1)$$

The resulting distribution is shown in Figure 1 as black dots. Figure 2 shows the event distribution from the H_2 target in the $\log_{10}\mathcal{P}$ vs. E_{CAL}/ν plane for all events (a); inelastic events, as determined by the second method

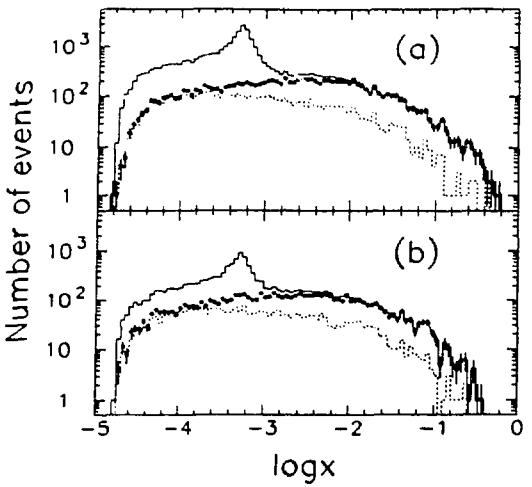

Figure 1. Event distribution vs. $\log_{10} x$ from H_2 (a) and D_2 (b) after kinematic cuts only (solid line), kinematic and calorimeter cuts (black dots) and kinematic cuts plus the hadron requirement (dotted line).

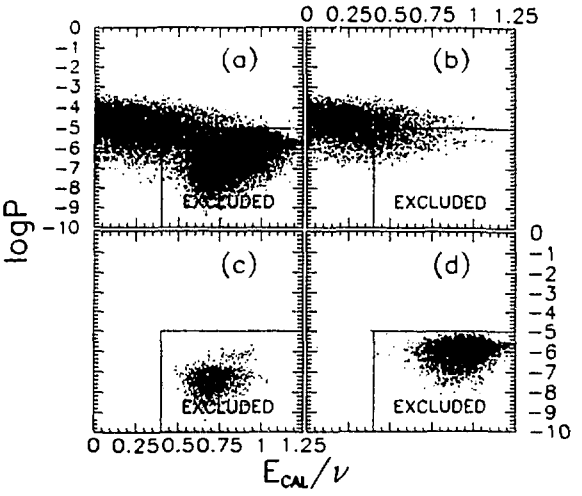

Figure 2. $\log_{10} \mathcal{P}$ vs. E_{CAL}/ν for all events (a) and for three different event types, inelastic, bremsstrahlung and μe, classified without use of the calorimeter (b)–(d).

below (b); μ-bremsstrahlung events, events with $x < 10^{-4}$ and no additional tracks besides the scattered muon (c); and elastic μe events, identified as events with only one muon and one negative secondary track in the final state (d). The distributions from the D_2 target look very similar. It can be seen that the cuts remove essentially all electromagnetic events of either type, while most inelastic events are retained.

In the second method, inelastic events were explicitly selected by requiring at least two hadrons of the same sign to be associated with the event. Here a "hadron" was defined as any reconstructed track compatible with coming from the event vertex, other than the scattered muon or other muons. The same-sign requirement was imposed to avoid contamination from γ photons converting into e^+e^- pairs. The result is shown in Figure 1 as a dotted line. At low x, similar numbers of events are selected by the two methods. At higher x, however, the number of events with the second method is much smaller, due to smaller ν values and because of smaller acceptance for low-momentum tracks in the forward spectrometer.

RESULTS

The ratio σ_n/σ_p is derived from the event yields from the H_2 and D_2 targets and the target densities and beam fluxes, assuming $\sigma_d = (\sigma_p + \sigma_n)/2$ and correcting only for events originating in the target vessel and a $\sim 5\%$ contamination of the D_2 target with HD molecules. In particular, no corrections were applied for Fermi motion, the effect of which is expected[8] to be negligible at $x < 0.6$, or nuclear shadowing effects in the deuteron. Also, no radiative corrections were performed, other than the removal of the backgrounds described above. The remaining radiative corrections on the ratio are not expected to be large.

Figure 3 shows the ratio σ_n/σ_p as a function of x, as derived by the two methods, the calorimeter cuts (full dots) and the hadron requirement (exes). Only statistical errors are

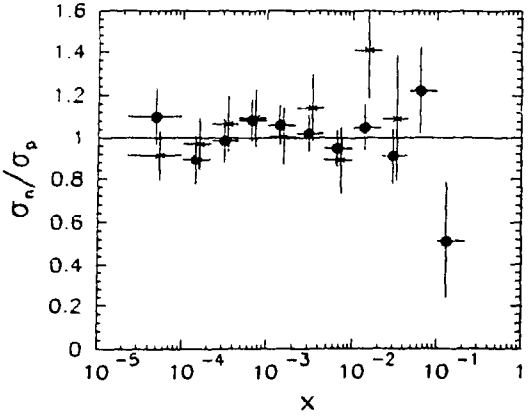

Figure 3. σ_n/σ_p with calorimeter cuts (•) and hadron requirement (×). The vertical error bars show the statistical errors and the horizontal the extend of the x bins. The two sets of points are slightly displaced for clarity.

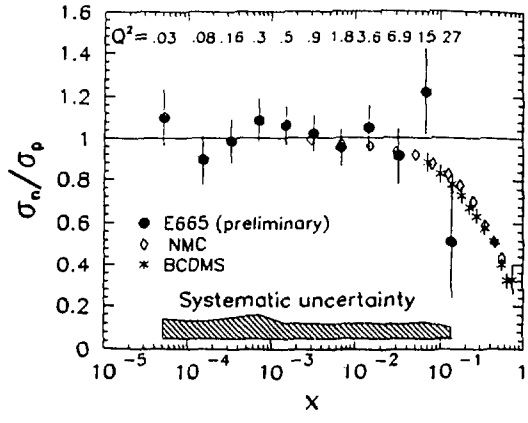

Figure 4. Preliminary results on σ_n/σ_p vs. x (•). The error bars show the statistical errors, while the shaded band shows the estimated systematic uncertainty. Also shown are previous results on F_2^n/F_2^p from NMC[5] (◇) and BCDMS[9] (×).

shown. The two sets of points are slightly displaced for clarity, with the horizontal bars showing the extend of the x bins. The two methods give compatible results, within the statistical uncertainties, giving confidence that the electromagnetic backgrounds have been removed properly. The results from the first method will be used, because of the better statistics, especially at higher x.

Systematic errors include a ±2% uncertainty on the relative beam fluxes and a ±3% uncertainty on the relative acceptance for the two data samples, which were taken at different running periods. These translate into a ±7% total normalization uncertainty on σ_n/σ_p. As a further check on the relative normalization, the cross-section ratio for elastic μe scattering from the D_2 and H_2 targets was measured to be 1.01 ± 0.03, consistent with 1.

The calorimeter was cross-calibrated for the two data-taking periods using electrons from elastic μe events. The uncertainty in the subtraction of the electromagnetic backgrounds due to residual differences in the calorimeter response were included in the systematic error. This uncertainty is sizable only at $x < 10^{-3}$.

Figure 4 shows the ratio obtained with the calorimeter cuts (black dots). The band at the bottom of the plot shows the estimate for the size of the systematic uncertainties. The average Q^2 value in each x bin is shown at the top of the plot. The W of the data (the invariant mass of the hadronic final state) is always greater than 10 GeV, far above the resonanse region, with an average varying from 25 GeV at the lowest x to 12 GeV at the highest.

Also shown in Figure 4 are the results for F_2^n/F_2^p from the two highest-statistics previous experiments, NMC[5] (open diamonds) and BCDMS[9] (exes). This structure-function ratio is equal to the cross-section ratio if the ratio R of transverse-to-longitudinal cross sections for the proton and neutron are equal, as suggested by an analysis of data from SLAC[10] at higher x, and assuming that the radiative corrections affect the two targets equally. These corrections are still under investigation.

The effect of nuclear shadowing on deuterium is at present unknown, as no experi-

mental measurements exist. Calculations[11,12] predict an effect of up to $2-4\%$ at some values of x and Q^2, but these calculations do not extend to the kinematic range of this experiment. If the effect exists, the true values of σ_n/σ_p are higher than presented here.

DISCUSSION

The new results extend the low-x range of the measurement by two orders of magnitude. The ratio is equal to 1, within errors, throughout this range, consistent with the extrapolation of the NMC measurement. The validity of this extrapolation was crucial for the derivation[5] of the integral of the difference $F_2^p(x)-F_2^n(x)$ and the conclusion that the Gottfried sum rule[13] is violated. The present data bridge the gap between the high-x, high-Q^2 deep inelastic scattering data[5] and those from real photoproduction[6] at lower ν.

The equality of the neutron and proton cross sections for $x \rightarrow 0$ is expected from Regge arguments.[1,3] Our result is consistent with this expectation, provided any shadowing effects are small compared to the experimental uncertainties. Alternatively, if this equality is assumed to be true, then the above result suggests the absence of significant nuclear shadowing effects in the deuteron, whithin the statistical and systematic uncertainties.

REFERENCES

1. B. Badelek *et al.*, "Small x Physics," DESY Report No. DESY 91-124, 1991 (to be published).
2. E. Levin, "Nucleon Structure Functions at Small x," DESY Report No. DESY 91-110, 1991 (to be published).
3. B. Badelek and J. Kwieciński, "Electroproduction Structure Function F_2 in the low Q^2, low x region," *Phys. Lett.* (to be published).
4. P. Amaudruz *et al.*, "Proton and Deuteron F_2 Structure Functions in Deep Inelastic Muon Scattering," *Phys. Lett.* (to be published).
5. P. Amaudruz *et al.*, "Gottfried Sum from the Ratio F_2^n/F_2^p," *Phys. Rev. Lett.* 66, pp. 2712–2715, (1991).
6. D. O. Caldwell *et al.*, "Total Hadronic Photoabsorption Cross Sections on Hydrogen and Complex Nuclei from 4 to 18 GeV," *Phys. Rev.* D7, pp. 1362–1383 (1973).
7. M. R. Adams *et al.*, "A Spectrometer for Muon Scattering at the Tevatron," *Nucl. Instrum. Methods* A291, pp. 533–551, (1990).
8. L. L. Frankfurt and M. R. Strickman, "New Direct Way of Checking the Nuclear Core Hypothesis in Inclusive Hadron Scattering off the Polarized Deuteron," *Phys. Lett.* B76, pp. 285–288, (1978).
9. A. C. Benvenuti *et al.*, "A Comparison of the Structure Functions $F_2(x,Q^2)$ of the Proton and the Neutron from Deep Inelastic Muon Scattering at High Q^2," *Phys. Lett.* B237, pp. 599–604, (1990).
10. L. W. Whitlow *et al.*, "A Precise Extraction of $R = \sigma_L/\sigma_T$ from a Global Analysis of the SLAC Deep Inelastic e–p and e–d Scattering Cross Sections," *Phys. Lett.* B250, pp. 193–198, (1990).
11. B. Badelek and J. Kwieciński, "Shadowing in Inelastic Lepton-Deuteron Scattering," *Nucl. Phys.* B370, pp. 278-298, (1992).
12. V. R. Zoller, "Nuclear Shadowing in Deuteron and the Gottfried Sum Rule," *Phys. Lett.* B279, pp. 145-148, (1992).
13. K. Gottfried, "Sum Rule for High-Energy Electron-Proton Scattering," *Phys. Rev. Lett.* 18, pp. 1174–1177, (1967).